Received 25 August 2025, accepted 17 August 2026, date of publication 30 September 2026
www.computingonline.net / computing@computingonline.net

Print ISSN 1727-6209
Online ISSN 2312-5381
DOI 10.47839/ijc.25.3.4848

Single-Lead ECG Images Processing and Classification using Machine Learning

ROMAN MELNYK, TETYANA KOROTYEYEVA, ROMAN KUTELMAKH

Lviv Polytechnic National University, Ukraine,
ramelnyk@polynet.lviv.ua, tetyana.o.korotyeyeva@lpnu.ua, roman.k.kutelmakh@lpnu.ua, http://pz.lp.edu.ua

Corresponding author: Tetyana Korotyeyeva (e-mail: tetyana.o.korotyeyeva@lpnu.ua).

ABSTRACT This work presents an approach to processing single-channel ECG images cropped from a 12-lead protocol recorded by a cardiograph. The paper presents an approach to ECG analysis by working on the printed signals generated by the electrocardiograph. The classic approaches use the signals themselves, not the printed signals. The ECG image processing includes algorithms such as thresholding, thinning, flood filling, clustering, subtraction, and others. After noise and background removal, the ECG image is converted to binary, with only black and light yellow. This helps determine a baseline for partitioning a signal into two parts: upper and lower. The goal of processing is to identify the time intervals and geometric regions that distinguish, recognize, and classify ECG graphs. Image processing algorithms determine the heart rate and rhythm regularity, as well as depressions and elevations in the signal period. The extracted data are used for training and testing a known neural network for classifying ECG signals.

KEYWORDS ECG signal; abnormality; base line; depression; elevation, probability/coordinates histogram, clustering, subtraction, comparison, classification, Machine Learning.

I. INTRODUCTION

Today, many publications are devoted to the recognition and classification of ECG signals, showing various cardiac abnormalities in patients. Large datasets of different types of ECGs have also been collected for possible use of artificial intelligence tools.

The presented article reviews more than 20 examples of such works. None of them directly overlap with the proposed approach, since most of the articles consider the digital representation of an analog signal and use various classical methods for its processing.

This work considers ECG signals as visual patterns of printed images and uses image processing algorithms to obtain data for their classification.

This is the main novelty of the work. The article proposes a new idea: extracting the main characteristics of the printed curves of an ECG signal. The work attempts to simulate the actions of a doctor who, upon receiving an ECG image, analyzes the signal curves. The work does not aim to compete with approaches that process large datasets using neural networks. On the contrary, it processes the ECG image and classifies the extracted data using limited computational resources.

The proposed image processing mechanisms are relatively simple, but complexity is not a guarantee of better results. The use of simpler neural networks is also not a disadvantage if they demonstrate good results. Lightweight software tools can be implemented more easily on less powerful hardware. This is one of the motivations for developing printed ECG signal-processing algorithms, using lightweight neural networks and combining them into a single software package, for example, for a smartphone.

II. RELATED WORKS ON ECG SIGNAL IMAGE PROCESSING

The number of publications devoted to various aspects of electrocardiogram analysis has been large for 10-15 years. In the earlier part of this period, most works used various signal transformation methods. Later, artificial intelligence methods were applied to signal recognition. The development of analysis methods can be observed in the following review publications [1-3]. They considered various methods such as Fast Fourier Transform, Wavelet Transform, etc.

Although the main difficulty in processing ECG signals is the accurate identification of various parameters (such as P-, Q-, R-, S-, T-waves), a specific processing model implemented in LabVIEW was considered in [4].

Works [5-7] presented filters, methods for extracting the most important cardiac features, and multi-label ECG datasets for machine learning applications.

Papers [8, 9] described the use of signal filtering for electrocardiograms (ECG) for removing 50 Hz power-line interference and high-frequency noise components from the ECG signal. The algorithms are based on statistical and differential mathematical methods or the Normalized Least Mean Square (NLMS) algorithm.

In [10, 11], deep features and machine learning integration were discussed. A DNN model was trained on a dataset of more than 2 million labelled patterns to recognize 6 types of abnormalities in twelve-lead ECG signals. A variant of the complex wavelet transform, called a scatter transform, was incorporated in a deep residual neural network (ResNet) [12, 13].

In [14], data from multiple institutions worldwide were collected. A novel evaluation metric was proposed that accounts for different types of misclassification errors. In [15], benchmarking results were added for the freely accessible PTB-XL dataset. In [16], 131,149 twelve-lead ECG recordings from ten international sources were collected.

In [17], an algorithm for ECG pre-annotation and beat-to-beat separation for heartbeat classification using autoencoders was proposed. A software product for analyzing ECG signals is advertised on the website [19]. A tool is proposed for determining characteristics of 12-lead ECG signals.

III. ECG SIGNAL IMAGE PREPROCESSING

The standard twelve-lead electrocardiogram (ECG) is a widely used tool for monitoring cardiac function and diagnosing heart disease. When examining a patient who has undergone an electrocardiographic examination, the family physician obtains an ECG image printed on a marked sheet of paper. An example of one is shown in Fig. 1.

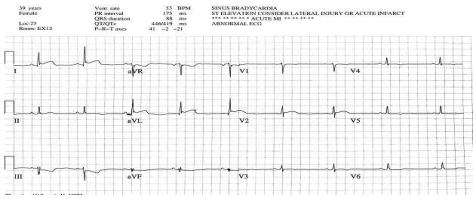

Figure 1. An image of the standard twelve-lead ECG signal from a cardiograph

Unfortunately, the protocol does not provide standardized reference ranges for characteristics, as in blood analysis protocols.

Based on the above features, abnormal ECG signals can be categorized into two classes: temporal deviations and shape (amplitude) deviations. In [20], heart diseases are classified based on various deviations from the normal signal.

The ECG signal image recorded by a standard device is not very clear, and on paper, it is superimposed on the ECG paper grid. A fragment of such a signal is shown in Fig. 2 (three R-waves from lead I).

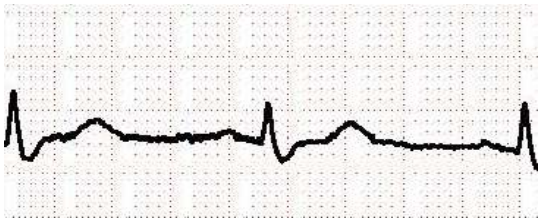

Figure 2. A fragment of an ECG plot on paper from a standard device

Experienced doctors use the full set of these ECG signals to make preliminary assessments of cardiac condition. This representation of the signal contains information that is not used by the algorithms. At the same time, some necessary information is lost due to the relatively large thickness of a recorder trace. There is no numerical representation.

For computer analysis, samples are cropped from one lead of the full 12-lead ECG signal. Other leads can be processed in parallel [21].

To obtain the model for investigation, the grid and other noise are removed by thresholding of the input image. The resulting image is then skeletonized using one of the known algorithms. The skeleton is marked in yellow (green for clearer illustration). These two new views of the signal are shown in Fig. 3.

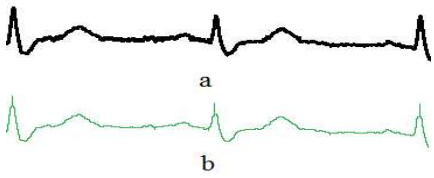

Figure 3. A transformed fragment of the ECG image (a) and its skeleton (b)

The thickness of the ECG trace is reduced. The plots in Fig. 4 illustrate this. This factor contributes to a more accurate determination of important points on the signal waveform.

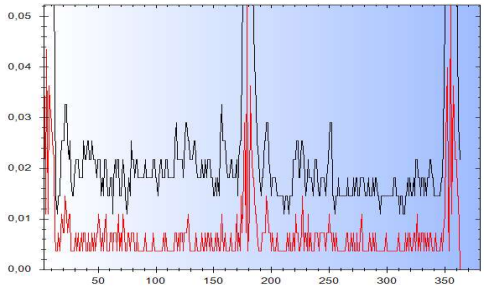

Figure 4. Thickness of signal lines: original (black) and thinned (red), OX - coordinates, OY - intensity

To stretch the graph along the OY axis, the upper part of the image with the yellow skeleton is filled with black, and the lower part with yellow using the flood-filling algorithm [23]. The resulting image (denoted as $I(\text{ecg})$) is shown in Fig. 5.

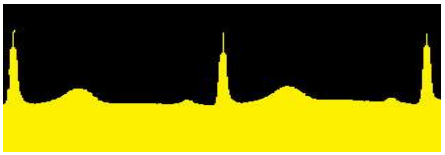

Figure 5. Filled regions of the ECG waveform

The filled image is useful for calculating the signal function and clustering to identify characteristics of this signal. Thus, the new ECG signal image with width W and height H is used to calculate the signal function:

$$y = f(x) = \frac{\sum_{i=1}^{H} b_{i,j}}{H}, \qquad 1 \le j \le W \qquad (1)$$

where $b_{i,j}$ is the intensity of a pixel in the i-th row and j-th column (0 or 200, black or yellow).

The new graph is more convenient for doctors and for further feature determination. Its thickness is one pixel; the waves are clearer, but the line fluctuates, reflecting the inaccuracies of the recording pen. Fig. 6 shows two ECG graphs: the original image, from the cardiograph, and the processed one.

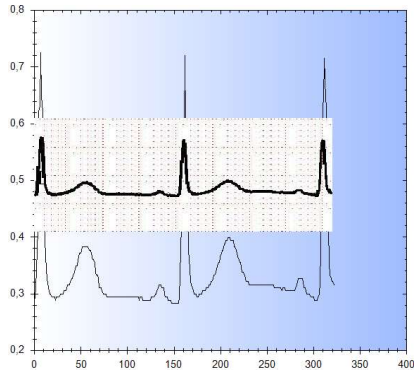

Figure 6. Two ECG graphs: original (black) and processed (thin), OX - coordinates, OY - intensity

The difference between the peaks and valleys of the graph is more noticeable if the difference between the intensity of the upper and lower parts of the signal image is greater. If the upper color is always black, then the difference between two values of the signal function depends on the values themselves and the intensity of the color used to fill the lower part:

$$D(i,j) = \{k_d(i,j) \times I(b)\}/H, \qquad (2)$$

where $I(b)$ is the intensity of the bottom part, $k_d(i,j)$ is the number of differing pixels between two columns i and j, and H is the number of rows (the height of the image).

IV. DETERMINATION OF TEMPORAL FEATURES IN ECG SIGNAL

The determination of the time intervals is carried out by isolating the main periodically repeated signal peaks. To do this, the columns of the image matrix are clustered as leaves. Their average intensities, calculated by formula (1), are elements that form clusters of columns with the same or similar intensities.

The K-means clustering algorithm is applied to W columns. For the task of selecting only R-wave coordinates, the number of output clusters is set to 2. Fig. 7 shows the input and output images for the normal ECG signal with four R-waves.

a b

Figure 7. Two ECG images: processed input (a) and clustered output(b)

The number of output clusters is set to 6-9 when selecting all other waves and segments. Fig. 8 shows the clustered image overlaid with the input image. The clusters are difficult to distinguish due to their superimposition with the input image.

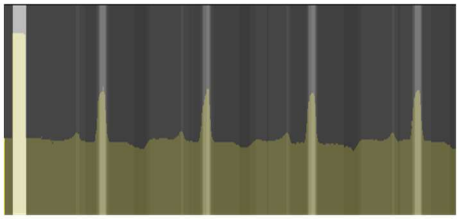

Figure 8. The ECG image superimposed on the clustered image

All temporal properties of waves and amplitudes are determined directly from the image. The advantages of this calculation compared with the input signal are as follows: there is no ambiguity in determining the coordinates (straight lines and right angles are available); there are no fluctuations on the graph, which simplifies finding the maximum and minimum values. The graph of the clustered image is calculated using formula (1) and shown in Fig. 9.

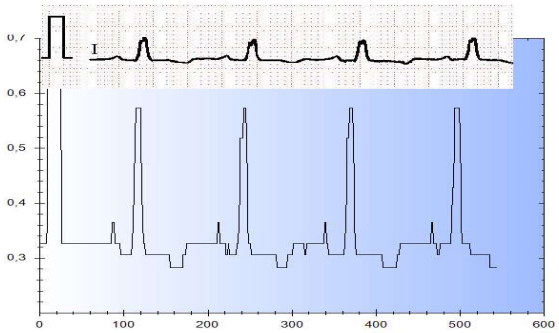

Figure 9. A graph of the clustered ECG image and the input ECG signal, OX -coordinates, OY -intensity

The original abnormal ECG signal from the cardiograph is also shown in Fig. 9. The approach is particularly useful if the signal contains high-frequency noise. The measurement accuracy is 1/8 of one small grid cell.

V. DETERMINATION OF ECG SIGNAL FEATURES

A. CONSTRUCTION OF A BASELINE IN AN ECG SIGNAL

In many cases, the features of ECG signals are primarily qualitative, including ST elevation, ST depression, reciprocal ST depression, T-wave inversion, hyperacute T-waves, and others. Examples of ECG signals with two different types of deviations are shown in Fig. 10. To distinguish the types of deviations, depression is marked in blue, and the elevation is marked in red.

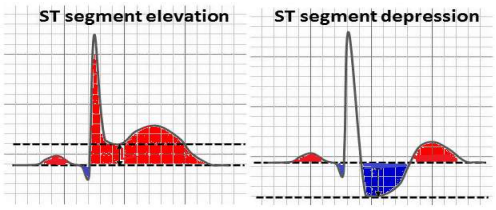

a b

Figure 10. ECG signals with ST segment elevation (a) and depression (b)

When recorded by a standard device, ECG signals may have slightly different baseline levels across different leads or intervals within the same lead. The K-means clustering algorithm can be used to form the baseline image. It is applied to the matrix rows (H is the number of rows). Fig. 11 illustrates these rows with increased row heights.

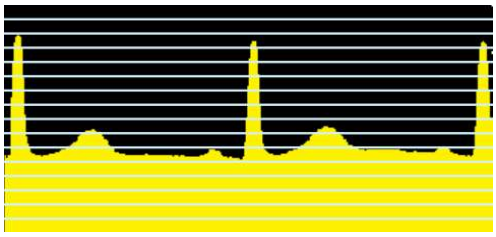

Figure 11. An image of the ECG signal with rows for clustering

For K=2, the algorithm divides the image into two parts: an upper dark part and a lower light part. For illustration, the clustered image is overlaid on the input image, and the resulting image is shown in Fig. 12.

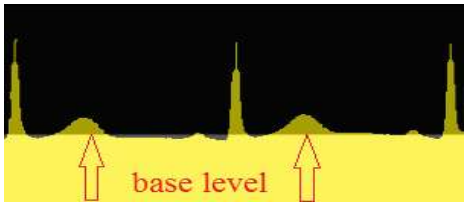

Figure 12. Division into two horizontal clusters

The image shows that the two periods of the original signal have slightly different levels due to measurement and recording inaccuracies.

For k=4, the distribution of pixels in clusters reflects the mean intensity of the clusters more accurately, and the baseline level is slightly lower. As a result, the image used to generate the baseline is ready for processing and shown in Fig. 13.

Figure 13. An image for baseline estimation

Then, the features characterizing the ECG signal are determined by subtracting the baseline image from the processed signal image:

$$I(\mathrm{d})=I(\mathrm{ecg})-I(0). \quad (3)$$

Pixels with equal values remain unchanged; the larger one (yellow>black) becomes red, and the smaller one (black<yellow) becomes blue. As a result, the difference image shows all the depressions and elevations of the original signal. They are marked with two colors in Fig.14: depressions are blue, and elevations are red.

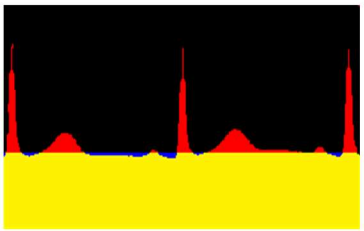

Figure 14. A difference image between the processed normal ECG signal and the baseline

The last operation completes the transformation of the signal image into a form with separated amplitude areas, ready for calculating the amplitude characteristics.

B. DETERMINATION OF ECG WAVEFORM FEATURES

Cardiac abnormalities are reflected in ECG waveforms. Some of them are very distinctive; others require experienced clinicians and additional data to decipher and identify subtle effects.

For a regular heart rate, the primary information about the cardiac condition is contained within one interval between two R-waves in each lead. It is repeated across all such intervals with some measurement variations.

To illustrate the approach, some known ECG signals are considered. In the first step, the normal and infarction ECG signals in lead I are chosen and shown in Fig. 15.

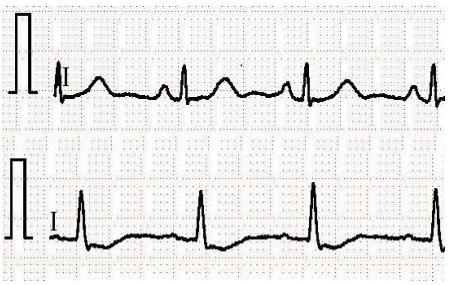

Figure 15. Normal and infarction ECG waveforms

For the first ECG image, a 1×10 grid is superimposed on the difference image (each period is covered with 5 equal fragments). Dividing the intervals of different ECG signals into the same number of fragments allows us to obtain characteristics of these signals with the same dimension, regardless of heart rate. In Fig. 16, the R-waves are excluded by marking them in pink.

A special histogram of pixels with a given intensity is constructed to find the coordinates of segments and their fill values (red and blue). It uses the probability/coordinate axes:

$$h(u,i)=\text{card}\{(u,v)\ /I(u,v)=i,\ u=1,2,\ldots,W,\ v=1,\ldots,H, \quad (4)$$

where $h(u,i)$ is the intensity frequency, $I(u,v)$ is the pixel intensity, u and v are the pixel coordinates, i is the pixel intensity for which the histogram is calculated, and W, H are the numbers of columns and rows.

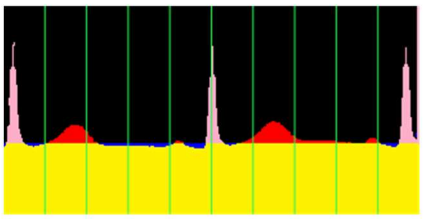

Figure 16. A difference image with fragments

For the two intervals and their average values, elevations and depressions of the normal signal have the following percentage contributions (the rounded values are calculated relative to all red and blue pixels, as shown in Table 1).

Table 1. Elevations and depressions in the normal ECG

Intervals	Fragments									
	1		2		3		4		5	
	blue	red	blue	red	blue	red	blue	red	blue	red
1	-3	0	0	+26	-5	+3	-6	+1	-2	+2
2	-1	+2	0	+35	0	+6	0	+4	-2	+1
Average	-2	+1	0	+31	-3	+4	-3	+3	-2	+1

Then, the average percentages of the ten color areas are represented in a histogram for the blue and red components. As a result, the new representation of the normal ECG signal is shown in Fig. 17.

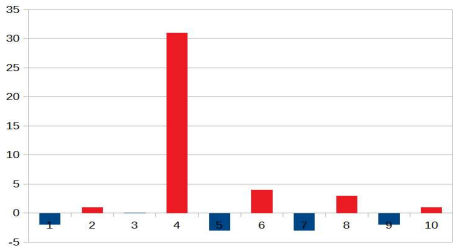

Figure 17. A histogram of color components in the difference image for the normal ECG, OX - fragments, OY – intensity

The same processing and calculations are performed on two other signals: infarction and abnormal ECG signals. The resulting images after processing are shown in Fig. 18.

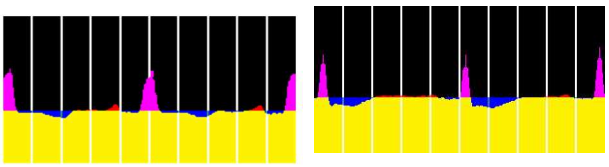

Figure 18. Difference images for infarction and abnormal ECGs

Their histograms are shown in Fig. 19. Some positions have a value of zero, as their average levels coincide with the baseline.

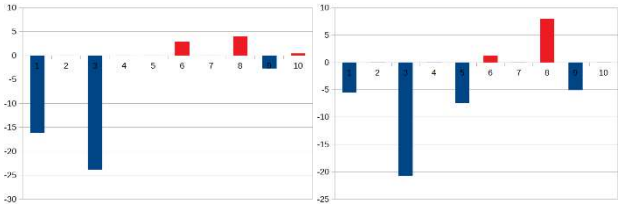

Figure 19. Histograms of colors for the infarction and abnormal ECGs, OX - fragments, OY - intensity

The last experiment conducted using the ischemia ECG signal is shown in Fig. 20.

Figure 20. An ischemia ECG signal

After the first stage of processing, the ECG image is shown in Fig. 21.

The main problem is that the space under the R-waves has no borders with the elevation area of the ST segment. To exclude this area, the K-means clustering algorithm is applied to W columns. Only two clusters are obtained: light in the locations of the R-waves and black in the remaining area.

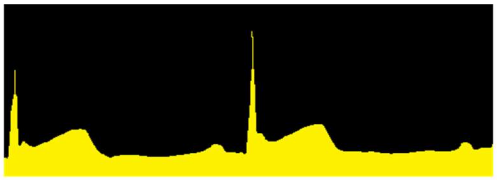

Figure 21. An ischemia ECG image

The R-waves are eliminated using the light cluster (two strips in Fig. 22).

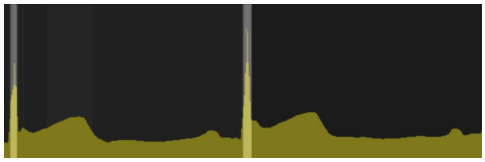

Figure 22. The input image overlaid with the clustered image

The resulting image for calculation of the signal features is shown in Fig. 23.

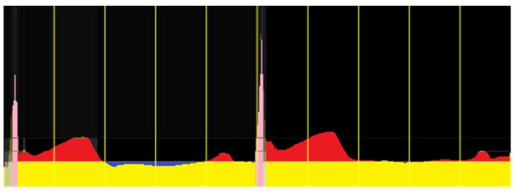

Figure 23. A difference image (ischemia ECG)

The average elevations and depressions of the ischemia signal in the two intervals are shown in the histogram in Fig. 24 (percentage values).

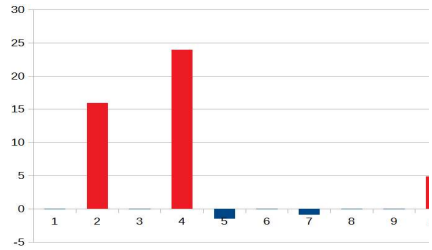

Figure 24. A histogram of colors in a difference image for the ischemia signal, OX - fragments, OY - intensity

In conclusion, a single-lead ECG image is processed to extract features similar to those that a cardiologist determines on an ECG graph to make a diagnosis, namely, the amplitudes of the waves, their relative location, and the depression or elevation of individual segments compared to normal.

VI. APPLICATION OF MACHINE LEARNING

The introduction above discusses many approaches that use deep learning based on different neural network architectures. A common feature of these works is the use of thousands of signal samples in datasets for training and testing the networks. Examples of such tools are TensorFlow [24] and Brain.js [25].

The approach below is based on data obtained after processing images of some typical and test signals. The data are time-independent and universal for all signal types and their parts in individual leads. To train and test the Brain.js neural network (feedback neural network), time intervals, data from histograms of signal difference images, namely: elevation and depression regions, as well as baseline regions, are used. Then, the machine learning software classifies ECG images immediately after the cardiogram is photographed according to the protocol received from the cardiograph. The basis for comparing the new input signal is a set of previously collected and processed known ECG signals.

Two models are developed for classification: the first by time intervals, and the second by their time-independent features. In the first case, the distance between the R-waves should fall within the interval 0.6-1.2 sec. Therefore, the training data has the form (-1, -1) for a time interval of less than 0.6 s (tachycardia) and (1, 1) for the time interval of more than 1.2 s (bradycardia). The test data has the form (1, -1) for the value within the required interval. Here, instead of just signs (+, -), the value 1 is used.

Thus, several operators for classification by the R-R distance, with two input values, are as follows:

```
const network = new brain.NeuralNetwork();
network.train( [
  {input:[1,-1], output:{normal:1}},
  {input:[1,1], output:{tachycardia:1}},
  {input:[-1,-1], output:{bradycardia:1}},
] );
let result = network.run([1,-1]);
document.getElementById("demo").innerHTML =
"normal: " + result["normal"] + "<br>" + "bradycardia:
" + result["bradycardia"] + "<br>" + "tachycardia:
" + result["tachycardia"];
```

The result of this simple code is predictable:

normal:0.9129508137702942,
bradycardia:0.04934118315577507,
tachycardia: 0.07432011514902115.

A simpler model is designed for classifying arrhythmias. Among the three R-R distances, the difference between the maximum and minimum values is calculated. Its relative value represents the deviation of the R-R distance, i.e., the degree of uniformity of the heart rate. When a tolerance for a normal heart rate is known, only its value and the R-R deviation of the input signal are required to classify the signal as arrhythmic.

The second model can contain as many objects as there are types of cardiograms that have been processed to obtain their characteristics. Each object can be described by all components of the histogram or only by its main part, which represents the ST segment. It is obvious that the larger the set of processed signals, the more components must be taken into account, while simultaneously increasing the number of parts into which the intervals between R-waves are divided.

In this example, four objects are considered:

F_t= *(-2, +1, 0, +31, -3, +4, -3, +3, -2, +1)* for the normal signal,
F_t= *(-16.1, 0, -23.8, 0, 0, +2.9, 0, +4, -2.7, +0.5)* for the infarction signal,
F_t= *(-6, 0, -21, 0, -7.5, +2, 0, +8, -5.5, 0)* for the abnormal signal,
F_t= *(0, +16, 0, +25, -2, 0, -1, 0, 0, +5)* for the ischemia signal.

To illustrate the logical flow of the application, only a few main JavaScript statements are shown below (the number of iterations and the error threshold are controlled):

```
const network = new brain.NeuralNetwork();
// Train the Network with 4 input objects
network.train( [
  {input:[-1.5, +0.8, 0, +32.0, -2.3, +4.2, -2.7, +2, -1.7,
    +1.1], output:{zero:1}},
  {input:[-16.1, 0, -23.8, 0, 0, +2.9, 0, +4, -2.7,
    +0.5],output:{one:1}},
  {input:[-5.5, 0, -20.8, 0, -7.5, +1.3, 0, +8, -5.1, 0],
    output:{two:1}},
  {input:[0, +16, 0, +25, -1.5, 0, -1, 0, 0, +4.5],
    output:{three:1}},],
{
  iterations: 50000,
  errorThresh: 0.002,
} );
```

To determine the type of a heart disorder the following statement is used:

```
let result = network.run( [-4.5, +0.8, -18, 0.3, -5, 1, 0, +6,
6.1, 0] );
```

The classification results are as follows:

infarction: 0.05449743941426277,
normal: 0.04030778259038925,
abnormal: 0.9158487915992737,
ischemia: 0.0017213531536981463.

As the main identification information is located in the first three fragments (three blue-red pairs) of the R-R interval, training and testing can be performed using their area values. By increasing the number of iterations to 100,000 and

decreasing the error threshold to 0.0002, more accurate classification results are obtained:

infarction: 0.013793044723570347,
normal: 0.016262317076325417,
abnormal: 0.9804368615150452,
ischemia: 0.000003827202817774378.

These experiments show that the greater the contrast in the input data, the more distinct the classification probabilities become. A conclusion should be drawn after repeating the same manipulations with the ECG signal in other leads and consulting a cardiologist.

In conclusion, the developed software, combined with machine learning, classifies four types of ECG signals based on elevation and depression in the ST segment as well as heart rate regularity.

VII. CONCLUSION

In this work, the input data are images, not digital values of an analog signal. Their processing involves algorithms such as thresholding, thinning, flood filling, K-means clustering, special subtraction, and others. The first two eliminate background, noise, and extra oscillations. The remaining algorithms simplify the determination of temporal properties, enhance the signal representation, and identify signal depressions and elevations.

The goal of the processing is to define temporal features and determine geometric regions by which ECG graphs can be distinguished, and by which they can be recognized and classified. Image processing algorithms extract the heart rate and its regularity, as well as the amplitudes of depressions and elevations in the signal interval.

The extracted data are used for training and testing a known neural network for classifying ECG signals. As image processing is not yet fully automated, it cannot be applied to contemporary datasets with thousands of examples. That is why only four of the widely known ECG signals were used as examples to demonstrate the robustness of the approach.

References

[1] A. Gacek, W. Predrycz, *ECG Signal Processing, Classification and Interpretation. A Comprehensive Framework of Computational Intelligence*. Springer-London, Dordrecht, Heidelberg, New York, 1st edition, 2012, 279 p. e-ISBN: 978-0-85729-868-3.

[2] R. Rajni, I. Kaur, "Electrocardiogram signal analysis-an overview," *International Journal of Computer Applications*, vol. 84, issue 7, pp. 22-25, 2013. https://doi.org/10.5120/14590-2826.

[3] T. Anbalagan, M. K. Nath, D. Vijayalakshmi, A. Anbalagan, "Analysis of various techniques for ECG signal in healthcare, past, present, and future," *Biomedical Engineering Advances*, vol. 6, 100089, 2023. https://doi.org/10.1016/j.bea.2023.100089.

[4] S. H. Abd, M. Ghanim, "ECG feature extraction and classification using robust technique for critical cardiac cases," *AIP Conf. Proc.,* vol. 3219, issue 1, 020113, 2024. *The 5th Int. Conf. on Buildings, Construction, and Environmental Engineering*, 23 November 2023, Amman, Jordan. https://doi.org/10.1063/5.0236830.

[5] R. K. Kapila Vani, B. Sowmya, S. R. Senthil Kumar, G. N. K. Suresh Babu, R. Reena, "An adaptive fuzzy neuro inference system for classification of ECG Cardiac Arrthymias," *AIP Conf. Proc.*, vol. 2393, issue 1, 020137, 2022. *Int. Conf. of Recent Trends in Science and Engineering*, 27–28 February, 2021, Krishnagiri, India. https://doi.org/10.1063/5.0079821.

[6] A. Salimi, S. V. Kalmady, A. Hindle, O. Zaiane, P. Kaul, "Exploring best practices for ECG signal processing in machine learning," arXiv:2311.04229, 2 Nov., 2023, https://doi.org/10.48550/arXiv.2311.04229.

[7] T. F. Romdhane, R. Ouni, M. Atri, "Multidatabase ECG signal processing," *Proceedings of the 5th International Conference on Advanced Technologies for Signal and Image Processing (ATSIP)*, 20 October 2020, Sousse, Tunisia. https://doi.org/10.1109/ATSIP49331.2020.9231880.

[8] J. Parak, J. Havlik, "Frequency detection methods," pp. 1-6, 2011. Available at: https://humusoft.cz/docs/papers/tcp2011/091_parak.pdf.

[9] Zia-ul-Haque, R. Qureshi, M. Nawaz, F. Y. Khuhawar, N. Tunio, M. Uzair, "Analysis of ECG signal processing and filtering algorithms," *International Journal of Advanced Computer Science and Applications*, vol. 10, no. 3, 2019. https://doi.org/10.14569/IJACSA.2019.0100370.

[10] A. K. Singh, S. Krishnan, "ECG signal feature extraction trends in methods and applications," *BioMedical Engineering OnLine*, vol. 22, 2023, https://doi.org/10.1186/s12938-023-01075-1.

[11] A. H. Ribeiro, M. H. Ribeiro, G. M. M. Paixao, D. M. Oliveira, P. R. Gomes, J. A. Canazart, M. P. S. Ferreira, C. R. Andersson, P. W. Macfarlane, W. Meira Jr, et al., "Automatic diagnosis of the 12-lead ECG using a deep neural network," *Nature Communications*, vol. 11, no. 1, pp. 1–9, 2020. https://doi.org/10.1038/s41467-020-15432-4.

[12] A. Natarajan, Y. Chang, S. Mariani, A. Rahman, G. Boverman, S. Vij, and J. Rubin, "A wide and deep transformer neural network for 12-lead ECG classification," Computing in Cardiology, vol. 47, pp. 1–4, 2020. https://doi.org/10.22489/CinC.2020.107.

[13] M. P Oppelt, M. Riehl, F. P. Kemeth, and J. Steffan, "Combining scatter transform and deep neural networks for multilabel electrocardiogram signal classification," *Computing in Cardiology*, vol. 47, pp. 1–4, 2020. ttps://doi.org/10.22489/CinC.2020.133.

[14] E. A. Perez Alday, A. Gu, A. J. Shah, C. Robichaux, A. K. I. Wong, C. Liu, F. Liu, A. B. Rad, A. Elola, S. Seyedi, et al., "Classification of 12-lead ECGs: the PhysioNet," *Computing in Cardiology Challenge*, 2020, Preprint, August 2020, https://doi.org/10.1101/2020.08.11.20172601.

[15] N. Strodthoff, P. Wagner, T. Schaeffter, and W. Samek, "Deep learning for ECG analysis: Benchmarks and insights from PTB-Xl," *IEEE Journal of Biomedical and Health Informatics*, vol. 25, no. 5, pp. 1519–1528, 2021. https://doi.org/10.1109/JBHI.2020.3022989.

[16] M. A. Reyna, N. Sadr, E. A. Perez Alday, A. Gu, A. J. Shah, C. Robichaux, A. B. Rad, A. Elola, S. Seyedi, S. Ansari, et al., "Issues in the automated classification of multilead ECGs using heterogeneous labels and populations," *Physiological Measurement*, vol. 43, issue 8, 2022. https://doi.org/10.1088/1361-6579/ac79fd.

[17] A. Benhamida, M. Kozlovszky, "A novel algorithm for automated human single-lead ECG pre-annotation and beat-to-beat separation for heartbeat classification using autoencoders," *Electronics*, vol. 11, issue 23, 4021, 2022. https://doi.org/10.3390/electronics11234021.

[18] S. G. Begum, E. Priyadarshi, S. Pratap, S. Kulshrestha, V. Singh, "Automated detection of abnormalities in ECG signals using deep neural network," *Biomedical Engineering Advances*, vol. 5, 100066, 2023. https://doi.org/10.1016/j.bea.2022.100066.

[19] AI that reads ECGs in seconds. [Online]. Available at: https://www.powerfulmedical.com/pmcardio-individuals.

[20] Dr. Tom Leach, "ECG Abnormalities," [Online]. Available at: https://almostadoctor.co.uk/encyclopedia/ecg-abnormalities.

[21] V. Gancheva, "Parallel computational approach for image filtering," *WSEAS Transactions on Signal Processing*, vol. 21, pp. 131-141, 2025. https://doi.org/10.37394/232014.2025.21.15.

[22] C. Lastre-Dominguez, V. Jimenez-Ramos, H. Azcaray-Rivera, E. Perez-Campos, J. Munoz–Minjares, Y. Shmaliy, "Denoising ECG signals using weighted iterative UFIR filtering," *WSEAS Transactions on Signal Processing*, vol. 19, pp. 148-157, 2023. https://doi.org/10.37394/232014.2023.19.16.

[23] R. Melnyk, T. Korotyeyeva, & Y. Levus, "Chains defects detection in a printed circuit board image by the plane partition and flood-filling of traces," *International Journal of Computing*, vol.22, issue 2, pp. 35-42, 2023. https://doi.org/10.47839/ijc.22.1.2877.

[24] An end-to-end platform for machine learning, [Online]. Available at: https://www.tensorflow.org/.

[25] Machine Learning in JavaScript, [Online]. Available at: https://www.w3schools.com/ai/ai_whatis.asp.

ROMAN MELNYK, *a Professor of Software Engineering Department, Institute of Computer Sciences and Information Technologies, Lviv Polytechnic National University. Scientific interests: fuzzy clustering, recognition of visual information*

TETYANA KOROTYEYEVA*, an Associate Professor of Software Engineering Department, Institute of Computer Sciences and Information Technologies, Lviv Polytechnic National University. Scientific interests: neural networks, recommendation systems.*

ROMAN KUTELMAKH *is a PhD in Technical Sciences, Associate Professor at the Software Department of Lviv Polytechnic National University. His research interests include algorithm analysis and design, high-performance computing, digital image processing.*